

AN UPPER LIMIT ON THE MASS OF THE BLACK HOLE IN URSA MINOR DWARF GALAXY

V. LORA¹, F. J. SÁNCHEZ-SALCEDO¹, A. C. RAGA² AND A. ESQUIVEL²

Draft version November 4, 2018

ABSTRACT

The well-established correlations between the mass of massive black holes (BHs) in the nuclei of most studied galaxies and various global properties of their hosting galaxy lend support to the idea that dwarf galaxies and globular clusters could also host a BH in their centers. Direct kinematic detection of BHs in dwarf spheroidal (dSph) galaxies are seriously hindered by the small number of stars inside the gravitational influence region of the BH. The aim of this Letter is to establish an upper dynamical limit on the mass of the putative BH in the Ursa Minor (UMi) dSph galaxy. We present direct N-body simulations of the tidal disruption of the dynamical fossil observed in UMi, with and without a massive BH. We find that the observed substructure is incompatible with the presence of a massive BH of $(2-3) \times 10^4 M_{\odot}$ within the core of UMi. These limits are consistent with the extrapolation of the $M_{BH}-\sigma$ relation to the $M_{BH} < 10^6 M_{\odot}$ regime. We also show that the BH may be off-center with respect to the center of symmetry of the whole galaxy.

Subject headings: galaxies: individual (Ursa Minor dwarf spheroidal) — galaxies: kinematics and dynamics — galaxies: dwarf — stellar dynamics

1. INTRODUCTION

Intermediate-mass black holes (IMBH; $M_{BH} \sim 10^2 - 10^4 M_{\odot}$) accreting gas from their surroundings have been postulated to explain the engines behind ultraluminous X-ray sources recently discovered in nearby galaxies (see Colbert & Miller 2005, for a review). IMBHs would fill the existing gap between stellar and supermassive black holes found in active galactic nuclei. According to the tight relation between M_{BH} and the central velocity dispersion σ (Gebhardt et al. 2000; Ferrarese & Merrit 2000; Tremaine et al. 2002), or between M_{BH} and the mass of the bulge (Magorrian et al. 1998), a natural place to look for these IMBHs are astrophysical systems less massive than normal galaxies, such as dense star clusters, globular clusters, and dwarf galaxies. If M_{BH} is correlated with the total gravitational mass of their host galaxy (Ferrarese 2002; Baes et al. 2003), central BHs should be an essential element in dark matter dominated objects -such as dwarf spheroidal (dSph) galaxies. Estimates of the mass of BH in these systems would be of great importance in completing the $M_{BH}-\sigma$ relation.

Direct and indirect searches for IMBH at the centers of globular clusters and small galaxies have been attempted (e.g., Gerssen et al. 2002, 2003; Valluri et al. 2005; Maccarone et al. 2005; Ghosh et al. 2006; Maccarone et al. 2007; Noyola et al. 2008). For instance, Noyola et al. (2008) have reported a central density cusp and higher velocity dispersions in their central field of the globular cluster ω Centauri, which could be due to a central BH ($M_{BH} \sim 4 \times 10^4 M_{\odot}$). However, a new analysis by Anderson & van der Marel (2009) and van der Marel & Anderson (2009) does not confirm the arguments given by Noyola et al. (2008), and provides an upper limit for the BH mass of $1.2 \times 10^4 M_{\odot}$.

There is sparse evidence that BHs could be present in at least some dSph. The Ursa Minor (UMi) dSph galaxy has

been also suspected to contain a BH of $\sim 10^6 M_{\odot}$ (Strobel & Lake 1994; Demers et al. 1995). Maccarone et al. (2005) discuss the possibility that the radio source found near the core of UMi is, in fact, a BH with a mass $\sim 10^4 M_{\odot}$.

In this Letter, we examine the dynamical effects of putative IMBHs in the core of dSphs on the very integrity of cold, long-lived substructure as that observed on the northeast side of the major axis of UMi. Although UMi has long been suspected of experiencing ongoing tidal disruption, regions with enhanced volume density and cold kinematics cannot be the result of tidal interactions (Kleyna et al. 2003, hereafter K03; Read et al. 2006; Sánchez-Salcedo & Lora 2007). This suggests that the secondary peak in UMi is a long-lived structure, surviving in phase-space because the underlying gravitational potential is close to harmonic (K03). Sánchez-Salcedo & Lora (2007) derived an upper limit on the mass and abundance of massive dark objects in the halo of UMi to avoid a quick destruction of the clump by the continuous gravitational encounters with these objects. In this work, we will assume that the dark halo is comprised of a smooth distribution of elementary particles and then study the disintegration of the clump, placing constraints on the mass of a possible central IMBH in UMi.

2. INITIAL CONDITIONS AND N-BODY SIMULATIONS

2.1. Ursa Minor and its clump

Ursa Minor, located at a galactocentric distance of $R_{gc} = 76 \pm 4$ kpc (Carrera et al. 2002; Bellazzini et al. 2002), is one of the most dark matter-dominated dSphs in the Local Group, with a central mass-to-light ratio $M/L \gtrsim 100 M_{\odot}/L_{\odot}$ (e.g., Wilkinson et al. 2004). The measured central velocity dispersion is 17 ± 4 km s⁻¹ (Muñoz et al. 2005) and the core radius of the stellar component along the semimajor axis is ~ 300 pc (Palma et al. 2003). UMi reveals several morphological peculiarities: (1) The shape of the inner isodensity contours of the surface density of stars appears to have a large ellipticity of 0.54, (2) the highest density of stars is not found at the center of symmetry of the outer isodensity contours but instead is offset southwest of center, (3) the secondary density peak on the northeast of the major axis is kinematically cold.

¹ Instituto de Astronomía, Universidad Nacional Autónoma de México, Ciudad Universitaria, Ap. 70-468, C.P. 04510 Mexico City, Mexico; vlora@astrocu.unam.mx, jsanchez@astrocu.unam.mx

² Instituto de Ciencias Nucleares, Universidad Nacional Autónoma de México, Ciudad Universitaria, Ap. 70-543, C.P. 04510 Mexico City, Mexico; raga@nucleares.unam.mx, esquivel@nucleares.unam.mx

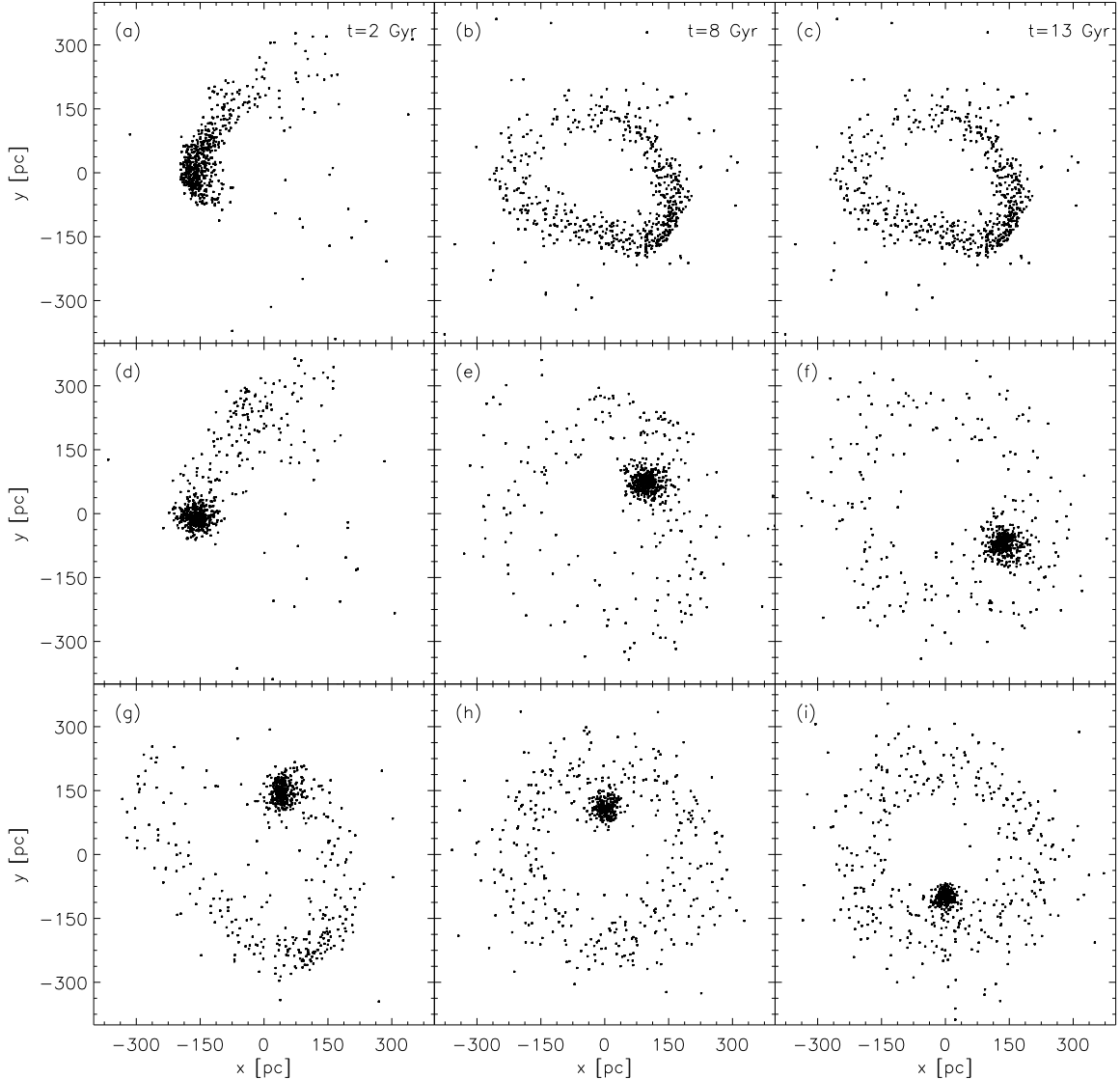


FIG. 1.— Snapshots at $t = 2, 8$ and 13 Gyr for $R_{1/2} = 50$ pc and $R_{\text{core}} = 510$ pc without self-gravity (top panel) and with self-gravity (middle panel). For comparison, the snapshots for $R_{\text{core}} = 300$ pc and with self-gravity are also shown (bottom panel).

The secondary density peak has a 1σ radius of $\simeq 1.6'$ (~ 35 pc at a distance of 76 kpc) when fitted with a Gaussian profile. The stellar distribution that forms this density excess is elongated not along the major axis of the isodensity contours of the elliptized King model, but along a line at an intermediate angle between the major and minor axes of these contours (Palma et al. 2003). The bend in the isodensity contours indicates that such clump is gravitationally unbound. Interestingly, K03 found that the velocity of stars within a $6'$ (130 pc) radius aperture on the clump are best fitted by a two-Gaussian population, one representing the underlying 8.8 km s^{-1} population, and the other with a line-of-sight velocity dispersion of 0.5 km s^{-1} . Although the value of the cold population is ill determined, we can be certain that the velocity dispersion is $< 2.5 \text{ km s}^{-1}$ at a 95% confidence level. The mean velocity of the cold population is equal to the systemic velocity of UMi, implying that either the orbit is radial and the clump is now at apocenter or the orbit lies in the plane of the sky (K03).

2.2. Initial conditions

We consider the evolution of a clump inside a rigid halo of dark matter with a density law:

$$\rho(r) = \frac{\rho_0}{\left(1 + [r/R_{\text{core}}]^2\right)^{1/2}}, \quad (1)$$

where ρ_0 is the central density and R_{core} is the dark halo core radius. This profile was chosen in order to facilitate comparison with K03. We explore different values for R_{core} . Following K03, once R_{core} is fixed, we rescale the central density to have a dark matter mass of $5 \times 10^7 M_{\odot}$ inside 600 pc, which is approximately the maximum extent of the stellar distribution observed in UMi. Therefore, in all our models, we have a total mass-to-light ratio of $(M_{\text{tot}}/L_V) \approx 90 M_{\odot}/L_V^{\odot}$ inside 600 pc, for a visual luminosity $L_V = 5.4 \times 10^5 L_{\odot}$ (Palma et al. 2003).

For a normal stellar population with $M/L_V = 2 M_{\odot}/L_V^{\odot}$, the stellar mass within the core radius of the dwarf is $\sim 4.5 \times 10^5 M_{\odot}$, whereas the dark matter mass is $> 6.2 \times 10^6 M_{\odot}$.

Therefore, the contribution to the potential of the baryonic mass was ignored.

The initial density profile of the clump follows a Plummer mass distribution,

$$\rho(r) = \frac{3}{4\pi} \frac{M_c R_p^2}{(r^2 + R_p^2)^{5/2}}, \quad (2)$$

where $M_c = 2 \times 10^4 M_\odot$ is the total mass of the clump and R_p is the Plummer radius. One should note that there is a simple relation for a Plummer model between R_p and the half-mass radius: $R_{1/2} = 1.3R_p$. We use $R_{1/2}$ values between 25 and 50 pc to initialize our simulations. The clump's self-gravity is included to have a realistic and complete description of its internal dynamics because, as we will see later, the tidal radius of the clump may be larger than $R_{1/2}$ when large values of R_{core} are used.

The clump is dropped at the apogalactocentric distance of 200 pc from the UMi center with a certain tangential velocity v_T , which defines the eccentricity e of the orbit. The orbit of the clump lies in the x - y plane, which is also the plane of the sky. For simulations with a central BH, it is clear that the evolution of the clump depends on its orbital eccentricity. For instance, we found that for a radial orbit, the BH dissolves the group of stars in its first passage through the galactic center. In order to provide an upper limit on the mass of the BH and since there is more phase space available for nearly circular orbits than for radial ones, we will take, in most of our simulations, a rather circular orbit with $e = 0.5$, which corresponds to $v_T = 5.7 \text{ km s}^{-1}$ for $R_{\text{core}} = 510 \text{ pc}$. However, to our surprise, the disintegration time was found to be insensitive to the initial eccentricity of the clump's orbit as long as $e < 0.87$. Altogether, there are essentially three model parameters that we have explored in our simulations: R_{core} , $R_{1/2}$ and M_{BH} .

2.3. *N*-body simulations

We developed an N -body code that links an individual timestep to each particle in the simulation. Only for the particle that has the minimum associated time, the equations of motion are integrated (with a second order predictor-corrector method). This "multi-timestep" method reduces the typical CPU time of direct, particle-particle integrations ($\propto N^2$, with N the number of particles), and allows integrations of systems of ~ 1000 particles to be carried out with relatively short CPU times.

The cluster density is so tiny that the internal relaxation timescale is very long ($\sim 11 \text{ Gyr}$ for an initial cluster with $R_{1/2} = 50 \text{ pc}$). Therefore, although our code is suitable to include two- and three-body encounters, the cluster behaves as collisionless and internal processes such as evaporation do not contribute to the dissolution of the cluster. For the same reason, all the particles have the same mass, and the presence of binaries was ignored.

All the simulations presented in this paper used 600 particles, each one having a mass of $33M_\odot$. We chose a smoothing length of 0.7 pc, which is approximately 1/10th the typical separation among cluster particles within $R_{1/2}$ at the beginning of the simulation. The convergence of the results was tested by comparing runs with different softening length and N . The effect of adopting a different smoothing radius between 0.1 and 1 times the typical distance was found to be insignificant. We run the same simulation with different N ($N = 200, 400, 600$ and 1800 particles), and convergence was found for $N \geq 400$.

In order to validate our simulations, we checked that, when the cluster evolves at isolation, the Plummer configuration is stationary and that the energy is conserved over 12 Gyr. To be certain that the interaction with the BH is resolved well, we compared the change in kinetic energy of the cluster, when colliding with a particle of mass $10^5 M_\odot$, moving at 200 km s^{-1} , with the predictions in the impulse approximation (Binney & Tremaine 2008), for different impact parameters, and found good agreement (differences less than 10%) between them.

We were also able to reproduce K03 simulations of the evolution of an unbound clump (ignoring self-gravity) in the gravitational potential created by the mass distribution given by Eq. (1). We confirm the K03 claim that even if the clump is initially very compact, with a 1σ radius of 12 pc, cusped halos cannot explain the survival of the substructure for more than 1 Gyr, while the substructure can persist for $\sim 12 \text{ Gyr}$ in halos with core radii 2–3 times the clump's orbit.

3. RESULTS

3.1. *Simulations without BH: the role of self-gravity*

We have first examined the evolution of a clump with $R_{1/2} = 50 \text{ pc}$ embedded in a galaxy with a large core of 510 pc (see Fig. 1). Note that when self-gravity is included, an initial $R_{1/2}$ value of $\sim 15 \text{ pc}$, as that used in K03, is no longer realistic because the clump remains too compact over its lifetime to explain its present appearance. With self-gravity, strong substructure continues to persist for a Hubble time, while in the non-self-gravitating case the substructure is completely erased in $\sim 10 \text{ Gyr}$. The evolution of the same self-gravitating clump but in a galaxy with $R_{\text{core}} = 300 \text{ pc}$ is also shown in Fig. 1. As expected, when the size of the galaxy core is decreased, the clump does not survive so long, but we can have a galaxy core of 300 pc without causing the clump to disintegrate in 13 Gyr. We confirm the K03 claim that cored halos allow the structures to remain uncorrupted for a Hubble time. Moreover, we find that, when including self-gravity, a galaxy core of 1.5 times the clump's orbit is enough to preserve the integrity of the clump.

3.2. *Simulations with BH*

If UMi hosts an IMBH, the density substructure is erased not only by the orbital phase mixing and the tidal field of the galaxy but also by the gravitational interaction with the hypothetical BH. Since the destructive effects depend on the mass of the BH, we can establish an upper limit on the mass of the BH in UMi by imposing that the BH must preserve the longevity of the clump for more than 10 Gyr. We proceeded to add a massive particle of $3 \times 10^4 M_\odot$ at the center of the galaxy potential, emulating a BH. Figure 2 shows the evolution of a self-gravitating clump with an initial size of $R_{1/2} = 50 \text{ pc}$ in a galaxy with $R_{\text{core}} = 510 \text{ pc}$. Under the influence of the gravitational pull exerted by the clump, the BH, initially at rest, is displaced from the center of UMi. The azimuthal orbital lag angle of the BH in the (x, y) plane is $\approx \pi/2$. As a consequence, the clump feels a gravitational drag and loses angular momentum which is transferred to the BH. Due to the angular momentum loss, the clump starts to spiral into the center. At 2 Gyr, we can see that, in fact, the clump has smaller orbital radius than it would have in the absence of the BH (see Fig. 2). The BH, on the other hand, spirals outwards to larger radii until it reaches its maximum galactocentric radius. At $t = 4 \text{ Gyr}$, the clump reaches the galactic center

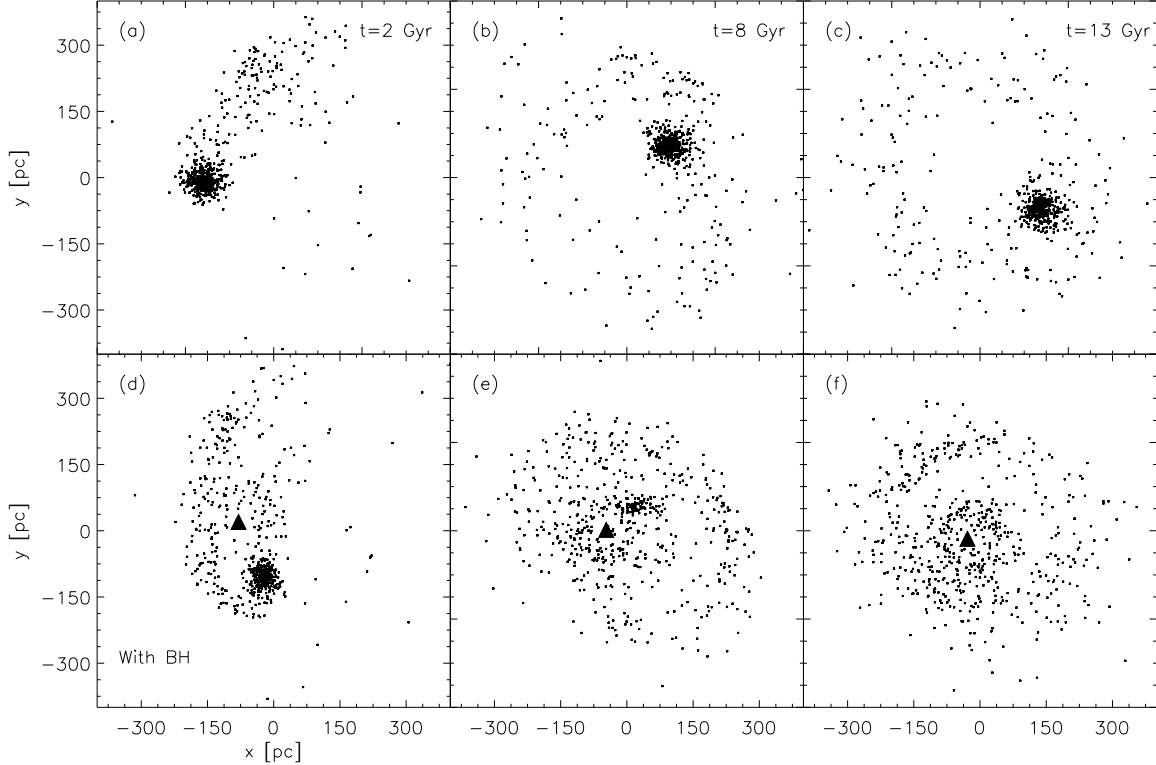


FIG. 2.— Snapshots at 2, 8 and 13 Gyr for a simulation with $R_{1/2} = 50$ pc and $R_{\text{core}} = 510$ pc (top panel), and the same simulation but with a BH (triangle) with mass $M_{\text{BH}} = 3 \times 10^4 M_{\odot}$ (bottom panel).

and this “exchange” of orbits starts all over again. Therefore, when looking at the BH of UMi, one should bear in mind that the BH does not necessarily settle into the center of the galaxy. It would be interesting to perform N-body simulations including the stellar background to elucidate if the two observed off-centered regions with the highest stellar density (e.g., Palma et al. 2003) are a consequence of the dynamical response to the BH. The minimum distance between the BH and the center of mass of the clump is ~ 100 pc in this model. Since the orbits of the clump and the BH never cross, the tidal disruption of the group of stars can be described as a secular process of stellar diffusion in phase-space. This slow relaxation process forms a stellar debris of stripped stars that move on a galactic orbit very similar to that of the clump itself.

In Fig. 2 we see that, under the influence of the BH, the clump is completely dissolved at 8 Gyr. In order to quantify the clump’s evolution, we calculated a map of the surface density of particles in the (x, y) plane at any given time t . We sample this two-dimensional map searching for the parcel (of 20×20 pc size) that contains the highest number of stars $\mathcal{N}_{\text{max}}(t)$. This region is centered at the remnant of the clump. The number of stars \mathcal{N}_{max} as a function of time is shown in Fig. 3. As expected, \mathcal{N}_{max} decreases as the simulation evolves due to the spatial dilution of the clump caused by tidal heating. Once \mathcal{N}_{max} drops a factor 2, which occurs in ~ 6 Gyr, the tidal disruption process is accelerated and \mathcal{N}_{max} dramatically declines at $\simeq 8$ Gyr (around the orbit 55), which can be taken as the disruption time, denoted by t_d . The disruption of the clump was confirmed by visual inspection of the simulations.

Further simulations show that even if the eccentricity of the orbit is similar to that of the isodensity contours of the surface density of UMi background stars, the disruption time is essentially the same.

We carried out simulations with $R_{1/2} = 50$ pc, $R_{\text{core}} = 510$ pc and $e = 0.5$, but with different M_{BH} . We found that the substructure disintegrates in 11 Gyr for a $10^4 M_{\odot}$ BH, and in 2 Gyr for $M_{\text{BH}} = 10^5 M_{\odot}$. We also explored different combinations for R_{core} and $R_{1/2}$. A reduction of the core of the galaxy leads to a more stringent upper limit on the mass of the BH. However, one can increase the longevity of the structure if a smaller value for $R_{1/2}$ is adopted. For instance, we also find that $t_d \simeq 8$ Gyr for $R_{\text{core}} = 200$ pc, $R_{1/2} = 25$ pc and $M_{\text{BH}} = 3 \times 10^4 M_{\odot}$.

In the absence of any knowledge about the initial dynamical state of the BH, the most natural assumption is that the center of the galaxy was its presumed birth site³. For completeness, we have also carried out simulations for an off-centered BH. A compilation of the models is given in Table 1. When the BH is on radial orbit, $t_d \simeq 4\text{--}9$ Gyr, for $M_{\text{BH}} = 3 \times 10^4 M_{\odot}$. Only in very special circumstances –when the BH is not on a radial orbit, the orbits are coplanar and the azimuthal lag angle is π –, the disruption of the cluster is less efficient because the separation between the clump and the BH is larger on average over the simulation.

We conclude that, if UMi’s clumpiness is a primordial artifact, then the survival of the secondary peak imposes an upper limit on the mass of the putative BH of $M_{\text{BH}} = (2\text{--}3) \times 10^4 M_{\odot}$, if the BH originally lurked at the center. The extrapolation of the $M_{\text{BH}}\text{--}\sigma$ relation for elliptical galaxies (Gultekin et al. 2009) predicts a $1.0 \pm_{0.9}^{5.0} \times 10^4 M_{\odot}$ BH for UMi. Therefore, our constraint is still consistent with both the extrapolated value and that inferred by Maccarone et al. (2005).

³ The BH candidate in UMi reported by Maccarone et al. (2005) is placed at about 7 pc from the center.

TABLE 1
RELEVANT PARAMETERS AND DESTRUCTION TIMES.

Run #	R_{core} pc	$R_{1/2}$ pc	BH position* at $t = 0$ [pc]	BH velocity at $t = 0$ [km s $^{-1}$]	M_{BH} M_{\odot}	t_d Gyr
0	510	50	—	—	0	> 14
1	510	50	0	0	5×10^3	> 14
2	510	50	0	0	1×10^4	11
3	510	50	0	0	3×10^4	8.3
4	510	50	0	0	1×10^5	1.7
5	200	25	0	0	3×10^4	7.8
6	510	50	(0,-50,0)	0	3×10^4	5.5
7	510	50	(0,0,-50)	0	3×10^4	8.5
8	510	50	(0,-50,0)	0	5×10^4	3.5
9	510	50	(0,0,-50)	0	5×10^4	5.0
10	510	50	(0,0,-50)	0	1×10^5	1.8

* The clump is initially at the position (200, 0, 0).

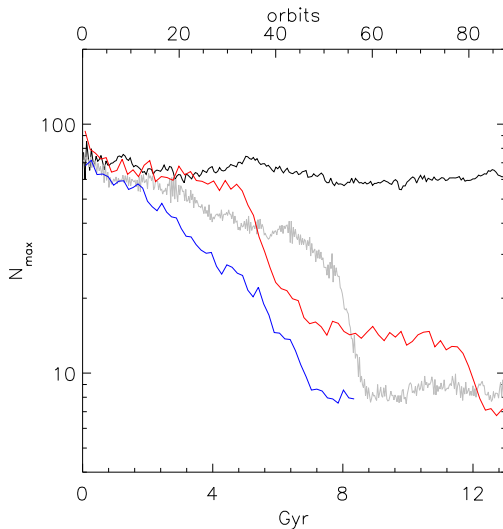


FIG. 3.— Smoothed curves of N_{max} as a function of time for runs # 0 (black line), # 3 (grey line), # 5 (red line) and # 6 (blue line).

4. DISCUSSION AND CONCLUSIONS

Our self-gravitating simulations confirm the claim of K03 that the dark halo of UMi must have a core radius of ~ 300 pc, comparable to the core radius of the underlying stellar population, in order to preserve the integrity of this clump. While the firm dynamical detection of an IMBH in any dSph galaxy is challenging because it requires observations of the velocity dispersion of stars deep into the core, we have demonstrated that the very integrity of kinematically cold substructure in dSph galaxies may impose useful limits not only on the core of the galaxy but also on the mass of putative BHs.

In the case of UMi, the maximum mass of a BH initially seated at the centre of the potential or initially on radial orbit, is $(2-3) \times 10^4 M_{\odot}$. When searching for direct detection of the possible IMBH in UMi (e.g., Maccarone et al. 2005), one should keep in mind that the BH may be offset from the galactic center because of the gravitational pull exerted by the clump.

As pointed out by the referee, the contour map of the surface brightness of the nucleus of M31 also has a bright off-center source (Fig. 2 of Lauer et al. 1993), which was interpreted not as a separate stellar system but as the apoapsis region of an eccentric stellar disk orbiting a central massive BH (Tremaine 1995; Lauer et al. 1996). The timing problem of the clump may be circumvented if one assumes that the secondary peak of UMi is the part of a ring close to apoapsis. Since the stars forming the secondary peak in UMi have a mean velocity equal to the systemic velocity of UMi, the ring should lie close to the plane of the sky and should be very eccentric. A serious difficulty with this scenario is that the apsides of the orbits need to be extremely aligned. Our simulations have shown that this alignment is not possible if the ring is the tidal debris of a stellar cluster. We do not know a satisfactory mechanism to explain the formation of a very eccentric stellar ring at scales of a galaxy with the required apsidal alignment.

The thoughtful comments and suggestions by an anonymous referee have greatly improved the paper quality. V.L., A.C.R. & A.E. thank financial support from grant 61547 from CONACyT. F.J.S.S. acknowledges financial support from CONACyT CB2006-60526 and PAPIIT IN114107 projects. V.L. wish to thank Stu group.

REFERENCES

- Anderson, J., & van der Marel, R. P. 2009, arXiv:0905:0627v1
 Baes, M., Buyle, P., Hau, G. K. T., & Dejonghe, H. 2003, MNRAS, 341, L44
 Bellazzini, M., Ferraro, F. R., Origlia, L., Pancino, E., Monaco, L., & Oliva, E. 2002, AJ, 124, 3222
 Binney, J. & Tremaine, S. 2008, Galactic Dynamics, Princeton Series in Astrophysics
 Carrera, R., Aparicio, A., & Martínez-Delgado, D. 2002, AJ, 123, 3199
 Colbert, E. J. M., & Miller, M. C. 2005, in The Tenth Marcel Grossmann Meeting. Eds. M. Novello, S. Perez Bergliaffa, & R. Ruffini, (Singapore: World Scientific Publishing), p. 530
 Demers, S., Battinelli, P., Irwin, M. J., & Kunkel, W. E. 1995, MNRAS, 274, 491
 Ferrarese, L. 2002, ApJ, 578, 90
 Ferrarese, L., & Merrit, D. 2000, ApJ, 539, L9
 Gebhardt, K., et al. 2000, ApJ, 539, L13
 Gerssen, J., van der Marel, R. P., Gebhardt, K., Guhathakurta, P., Peterson, R. C., & Pryor, C. 2002, AJ, 124, 3270
 Gerssen, J., van der Marel, R. P., Gebhardt, K., Guhathakurta, P., Peterson, R. C., & Pryor, C. 2003, AJ, 125, 376
 Ghosh, K. K., Suleymanov, V., Bikmaev, I., Shimansky, S., Sakhibullin, N. 2006, MNRAS, 371, 1587
 Gultekin, K., et al. 2009, arXiv:0903.4897v1
 Kleyana, J., Wilkinson, M., Gilmore, G., & Evans, W. 2003, ApJ, 588, L21 (K03)
 Lauer, T. R., et al. 1993, AJ, 106, 1436
 Lauer, T. R., et al. 1996, ApJ, 471, L79

- Maccarone, T. J., Fender, R. P., & Tzioumis, A. K. 2005, MNRAS, 356, L17
Maccarone, T. J., Kundu, A., Zepf, S. E., & Rhode, K. L. 2007, Nature, 445, 183
Magorrian, J., et al. 1998, AJ, 115, 2285
Muñoz, R. R., et al. 2005, ApJ, 631, L137
Noyola, E. & Gebhardt, K., & Bergmann, M. 2008, ApJ, 676, 1008
Palma, C., Majewski, S., Siegel, M., Patterson, R., Ostheimer, J., & Link, R. 2003, AJ, 125, 1352
Read, J., Wilkinson, M., Evans, W., Gilmore, G., & Kleyna, J. 2006, MNRAS, 367, 387
Sánchez-Salcedo, F. J., & Lora, V. 2007, ApJ, 658, L83
Strobel, N. V., & Lake, G. 1994, ApJ, 424, L83
Tremaine, S. 1995, AJ, 110, 628
Tremaine, S., et al. 2002, ApJ, 574, 740
Valluri, M., Ferrarese, L., Merritt, D., & Joseph, C. L. 2005, ApJ, 628, 137
van der Marel, R. P., & Anderson, J. 2009, arXiv:0905.0638v1
Wilkinson M. I., Kleyna J. T., Evans N. W., Gilmore G. F., Irwin M. J., Grebel E. K. 2004, ApJ, 611, L21